JOURNAL OF MATERIALS SCIENCE 32 (1997) 3349–3353

Conduction mechanisms in co-evaporated mixed Mn/Sio$_x$ thin films

S. Z. A. ZAIDI, J. BEYNON, C. B. STEELE*
Department of Physics, Brunel University, Uxbridge, UB8 3PH, UK

The thermoelectric power and d.c. conductivity of co-evaporated Mn/SiO$_x$ films, 100 nm thick, containing 20 to 100 at% Mn have been measured over the temperature ranges 275 to 580 K and 110 and 575 K, respectively. Three conduction regions have been identified: p-type, via non-polaronic holes and small polarons; intrinsic and metallic. The d.c. conductivity arises from a combination of non-activated and activated processes.

1. Introduction

Compared with pure metallic films, thin "cermet" films display some interesting electrical properties. These include a widely varying resistivity and temperature coefficient as a function of composition, and high stability when exposed to normal atmospheric conditions. The presence of the dielectric provides a considerable degree of passivation and temperature stability. Mn/SiO$_x$ films are not strictly cermets because they do not consist of two discrete phases throughout the whole composition range; silicide compounds may also be present [1]. Although various insulators can be used SiO$_x$ has proved popular because it can be readily deposited by thermal evaporation.

The characteristics of the films depend strongly on the technique employed and the deposition parameters: film thickness, substrate temperature, deposition rate and residual pressure. Various techniques have been used: thermal evaporation, sputtering (d.c., RF, magnetron), electron beam evaporation, etc.; the co-evaporation technique has been used for preparing Mn/SiO$_x$ films for the present investigation. It has the advantage over single-boat evaporation in that deposition parameters can be closely controlled and, as a result, film properties are more reproducible.

Mn/SiO$_x$, Cr/SiO$_x$, Cu/SiO$_x$ and Au/SiO$_x$ have been studied extensively in this laboratory. Results on Mn/SiO$_x$ prepared by single-boat evaporation have been obtained by a number of previous workers [2–4]; the investigations include d.c. and a.c. conductivity, thermoelectric power, optical absorption and structural analysis. However, no detailed comparison of conductivity/thermoelectric power has been presented for co-evaporated Mn/SiO$_x$ films. The nature of the dominant charge carriers can be obtained from thermoelectric power measurements, whilst the kind(s) of conduction mechanisms present in the films can be determined if d.c. conductivity and optical absorption data are also used.

There are two techniques for obtaining thermoelectric power data: the integral and differential methods [5]. A characteristic of the integral technique is that one junction is maintained at constant temperature whilst the temperature of the other is varied. It also allows samples of extended length ($\sim$ 3 to 5 cm) to be used. However, as the length of the sample increases the resistance also increases. This can be a disadvantage (as in the present study) where high concentrations of SiO$_x$ were used, producing highly resistive films. Accurate measurement of the Seebeck voltage can be difficult with the integral method because the measuring instrument possesses a substantial loading error. This problem can be overcome using the differential technique and short samples ($\sim$ 1 cm).

2. Experimental procedure

Mn/SiO$_x$ films of various compositions (20 to 100 at% Mn) were deposited from two tantalum boat-shaped filaments by co-evaporation using 99.9% pure manganese flake (Johnson & Mathey, Materials Tech., UK) and 99.9% pure select grade/vacuum baked silicon "monoxide" powder (Aldrich, UK) onto Corning 7059 alkali-free alumino-silicate glass substrates *in vacuo* $\sim$ 1.0 mPa.

The thermoelectric power samples possessed a planar geometry, 1.0 cm $\times$ 0.3 cm in size, whereas the d.c. conductivity samples possessed the traditional van der Pauw clover-shaped geometry with an active region of 0.3 cm $\times$ 0.3 cm. The Mn and SiO$_x$ were controlled using two calibrated quartz crystal oscillators. The mean deposition rate was 0.5 nm s^{-1} and the film thickness was 100 nm, as measured by multiple-beam interferometry with an Angstrometer (Sloan Instruments, Model M-100) and checked using an alpha-step R&D profilometer (Model 200, Tencor Instruments, UK). In all cases, aluminium was used as the electrode material.

* *Present address*: Directorate of Project Time and Cost Analysis, St Giles Court, London, WC2 8LD, UK.

0022–2461

Thermoelectric power, S, was measured using the differential technique in the temperature range 275 to 580 K. The Seebeck voltage was measured by a Keithley 617 programmable digital electrometer having an input resistance ~ 200 Tohm. A temperature difference of 10 K was maintained across the sample and four values of the Seebeck voltage were measured by altering the direction of the temperature gradient and reversing the polarity of the electrometer; an average value was obtained and S calculated from the slope of a graph of Seebeck voltage versus mean temperature. The d.c. conductivity measurements were performed using the standard van der Pauw technique [6] between 110 and 575 K. It was found necessary to cycle the temperature several times for both thermoelectric power (TEP) and d.c. conductivity until stable results were obtained.

Film composition was determined using X-ray photoelectron spectroscopy (XPS). XPS spectra were recorded with a VG ESCALAB 210 spectrometer (Fisons Surface Science) using AlK_α (1486.6 eV) radiation. Charge correction of the data was performed by referring to the carbon 1s peak at 284.6 eV. The residual pressure in the spectrometer during the analysis was better than 0.27 Pa.

3. Results and discussion

3.1. XPS

Experimentally-derived values of the core-level photoelectron binding energies as a function of composition are listed in Table I for 20 to 50 at % Mn films. It can be seen that the binding energies of the $Si(2p_{1/2})$ peak lie in the range 101.4 to 101.8 eV. These values do not coincide with the binding energies of either SiO (101.2 eV) or SiO_2 (103.1 eV) [7, 8]; there is a higher proportion of oxygen in the films than in silicon monoxide. The ratio of atomic concentration of oxygen to silicon oxide was calculated to be about 1.8, suggesting that the oxide is best represented by the formula Si_5O_9 [9]. XPS spectra of Mn/SiO_x films containing 20, 40 and 50 at % Mn all showed the presence of the C(1s) peak, most probably arising as a contaminant from rotary pump oil vapour during deposition.

3.2. Thermoelectric power

The relative thermoelectric power between a Mn/SiO_x film and an Al contact may be equated with the absolute thermoelectric power of the film because S_{Al} $(= -40\,nV\,K^{-1})$ is negligible compared with the experimentally determined values. Fig. 1a–c show how S varies with temperature for various compositions.

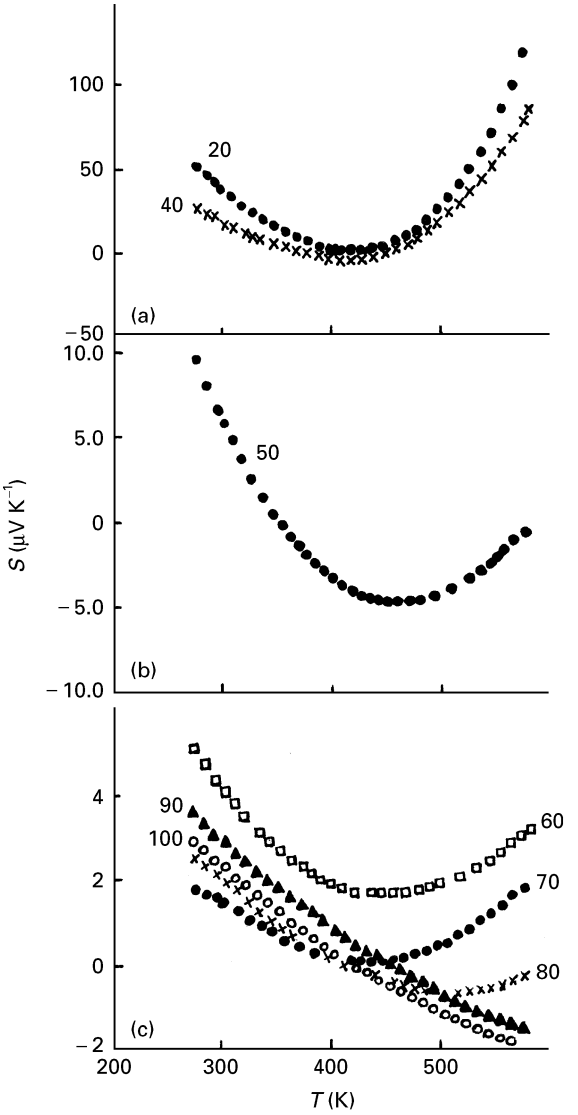

Figure 1 Variation of thermopower with temperature for different compositions (in at % Mn).

S consists of three regions: (i) S remains positive but decreases with increase in temperature up to 410 K for 20 at % Mn, 370 K for 40 at % Mn 355 K for 50 at % Mn, 460 K for 60, 70 and 100 at % Mn and 420 K for 80 and 90 at % Mn, indicating a p-type charge carrier conduction mechanism; (ii) S is negative between 370 and 450 K for 40 at % Mn and above 355 K for 50 at % Mn, 420 K for 80 and 90 at % Mn and 460 K in 70 at % Mn, indicating that intrinsic conduction is occurring; (iii) S becomes positive again and increases with increase in temperature above 410 K for 20 at % Mn, 450 K for 40 at % Mn and 460 K for 60 and 100 at % Mn, indicating metallic-like behaviour.

TABLE I XPS core level binding energies (in eV) of various compositions of co-evaporated Mn/SiO_x films

Mn (at %)	$Mn2s_{1/2}$	$Mn2p_{3/2}$	$Mn2p_{1/2}$	Mn3s	$Mn3d_{3/2}$	$Mn3p_{1/2}$	$O2s_{1/2}$	$O1s_{1/2}$	Si2s	Si2p
20	770.7	641.4	653.3	82.9	4.4	48.2	23.8	531.4	152.6	101.8
30	772.3	641.5	653.6	82.9	4.4	48.2	23.7	531.3	152.7	101.9
40	770.9	640.9	652.9	82.8	4.2	47.8	23.7	531.0		101.4
50	770.8	641.0	652.8	83.6	3.9	47.6	23.7	531.3		101.4

3.3. Conduction processes

3.3.1. p-type conduction

A positive TEP which decreases with increasing temperature suggests that a valence band transport mechanism is taking place via p-type carriers. The TEP, S_{val}, has the general form [10]

$$S_{val} = (k/e)[(E_f - E_v)/kT + f(T)] \quad (1)$$

where E_f is the Fermi energy, k is Boltzmann's constant, e is the electronic charge and T is the absolute temperature. E_v is taken to be the mobility-shoulder energy. The exact form of $f(T)$ is unknown but is assumed to be a slowly-varying function. In amorphous semiconductors, $f(T)$ only makes a small contribution to S_{val}. Thus, Fig. 1a–c suggest that holes in the valence band are the dominant charge carriers between 275 and 460 K, and Relation 1 is applicable. The charge carriers are non-polaronic holes for $E_\sigma(T) < E_s(T)$ whereas they are probably small polarons for $E_\sigma(T) > E_s(T)$. Fig. 2a–d display typical $E_\sigma(T)$ versus T and $E_s(T)$ versus T graphs. Table II lists the cross-over temperature T_{co} at which $E_\sigma(T) = E_s(T)$, the hopping energy $(E_\sigma(T) - E_s(T))$ and the nature of the carriers above and below T_{co}.

3.3.2. Intrinsic conduction

Depending on the donor and acceptor concentrations, electronic and hole conduction may become appreciable in narrow-band materials if the temperature is sufficiently high [11]. Intrinsic conduction occurs when the electron and hole concentrations are equal and the electron mobility is greater than the hole mobility. Since the sign of the thermoelectric power is negative, there is a strong similarity to an n-type semiconductor. The temperature range over which intrinsic conduction is occurring (obtained from Fig. 1a–c) is also given in Table III. The temperatures agree with that obtained (> 420 K) from Hall effect measurements in Au/SiO_x (2 at % Au) films [12]. In general, the thermoelectric power S_{int} can be expressed as [13]

$$S_{int} = [(S_p\sigma_p - S_n\sigma_n)]/(\sigma_p + \sigma_n) \quad (2)$$

where σ_n and σ_p are the respective contributions to the electrical conductivity from electrons and holes and S_n and S_p are the thermoelectric powers.

3.3.3. Metallic-like conduction

Table III lists the temperature region where the thermoelectric power is positive and increases with temperature. This metallic-like property may arise from the overlapping of an impurity and valence band. It had previously been observed in 10 at % Mn films above 500 K [14].

The thermoelectric power may be expressed as [15]

$$S_m = \pi^2 k^2 T/eE_f \quad (3)$$

although the value of the Fermi energy is usually smaller in degenerate semiconductors than in metals.

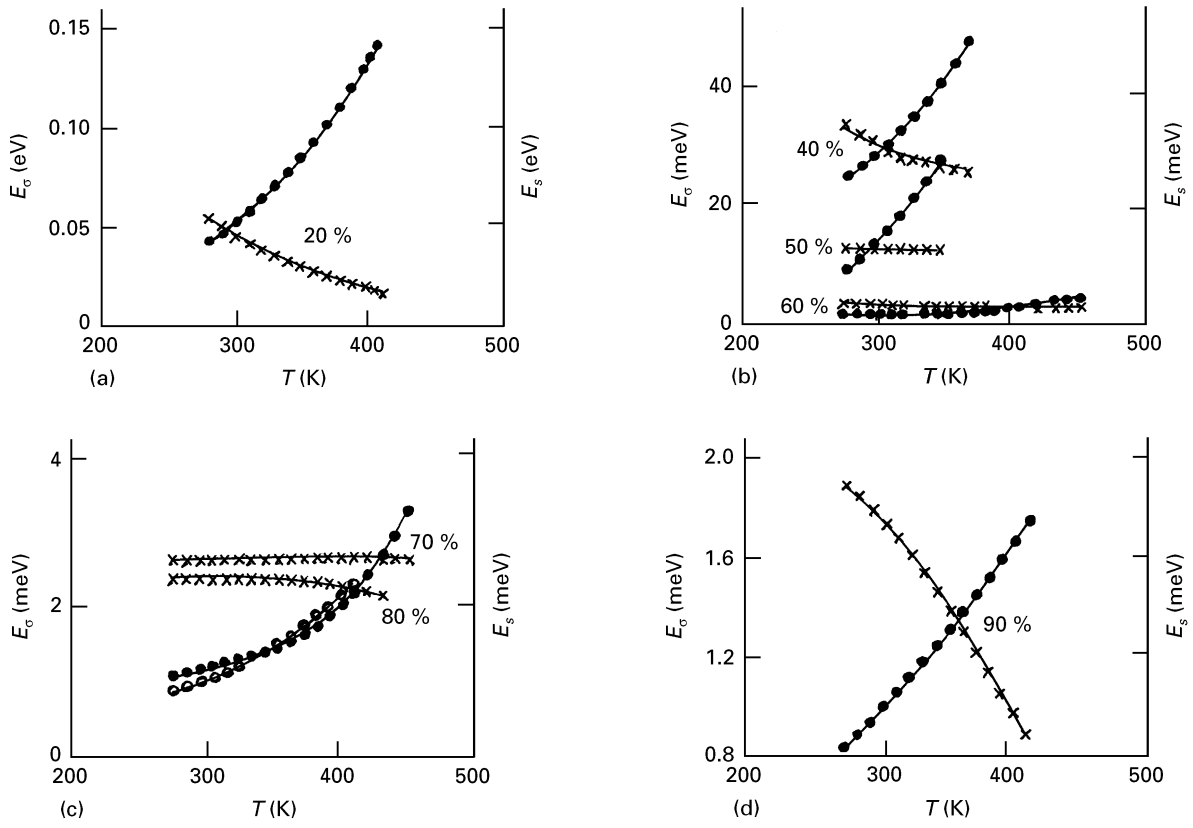

Figure 2 Variation of d.c. conductivity activation energy E_σ (●) and thermopower activation energy E_s (×) with temperature for different compositions (in at % Mn) (note: in (c) ○ is used for the 80% variation in E_s).

TABLE II Nature of charge carriers over various temperature ranges for co-evaporated Mn/SiO_x films

Mn (at %)	Temperature (K)					$(E_\sigma - E_s)$ Hopping energy (meV)
	Cross-over ($E_\sigma = E_s$)	p-type ($E_\sigma < E_s$) (non-polaronic holes)	p-type ($E_\sigma > E_s$) (small-polarons)	Intrinsic conduction (dominant electrons)	Metallic-like conduction (dominant holes)	
90	430	278–430	431–460	> 460	–	0 to 0.63 at 460 K
80	410	275–410	411–420	> 420	–	0 to 0.05 at 420 K
70	363	278–363	364–420	> 420	–	0 to 0.86 at 420 K
60	400	278–400	401–460	–	460	0 to 1.87 at 455 K
50	295	278–295	296–355	> 355	–	0 to 15.36 at 350 K
40	305	278–305	306–370	370–450	450	0 to 22.55 at 368 K
20	290	278–290	291–410	–	410	0 to 116.0 at 408 K

TABLE III Conduction mechanisms operating in co-evaporated Mn/SiO_x films at various temperatures

Mn (at %)	Temperature range (K)		
	Hopping conduction	Intrinsic conduction	Metallic-like conduction
1	258–360	360–558	558
3	258–360	360–558	558
5	258–360	360–558	558
10	278–500	–	500

4. D.c. conductivity

4.1. Non-activated conduction

The d.c. conductivity, $\sigma_{d.c.}$, for a p-type semiconductor may be written as

$$\sigma_{d.c.} = ep\mu \tag{4}$$

where p is the hole concentration and μ is the d.c. conductivity mobility. Under low field d.c. conditions and zero activation energy, Equation 4 may be rewritten as [16]

$$\sigma_{d.c.} = 2e^2R^2v_{ph}\,p\exp(-2\alpha R) \tag{5}$$

where R is the mean distance between impurity centres, v_{ph} is the phonon frequency and $1/\alpha$ is the localization length of the wave-function at an impurity centre. Equations 5 and 6 give

$$\mu = 2eR^2v_{ph}\exp(-2\alpha R) \tag{6}$$

which is independent of temperature.

Fig. 3 shows that the d.c. conductivity of films with 60 to 100 at % Mn is temperature-invariant, indicating that μp is also independent of temperature. (Also shown for comparison are the results for films containing < 50 at % Mn.) A similar result was found in Au/SiO_x films [12, 17]. If it is postulated that the carrier concentration, C_f, in most metal/insulator films is temperature-independent then μ will also be temperature-independent in 60 to 100 at % Mn films. C_f is expected to obey a relation of the form

$$C_f = C_{Al}\exp(Se/k) \tag{7}$$

where C_{Al} is the carrier concentration of the aluminium contact (taken to be 6.0×10^{22} cm^{-3} [18]).

The structure of films with > 60 at % Mn is primarily composed of metallic capillaries. $\sigma_{d.c.}$ varies with temperature according to a polynomial in $(T - T_0)$ of the kind

$$\sigma_{d.c.} = \sigma_0[1 + \alpha(T - T_0) + \beta(T - T_0)^2 + \ldots] \tag{8}$$

where σ_0 is the conductivity at temperature T_0 and α and β are constants.

4.2. Activated conduction

Fig. 3 shows that the d.c. conductivity has a non-linear dependence on temperature for 20 to 50 at % Mn films, which implies that there is no unique activation energy E_σ; E_σ increases monotonically with temperature. For example, with 10 at % Mn films at 293 K [14]

$$E_\sigma(\text{eV}) = 0.05 - 8.4\ 10^{-4}T + 3.2\ 10^{-6}T^2 \tag{9}$$

Below 60 at % Mn, the film has a predominantly island structure. $\sigma_{d.c.}$ is now best described by [16]

$$\sigma_{d.c.} = \sigma_0\exp[-\{E_f - E_{max}(T) - E_h(T)\}/kT] \tag{10}$$

where σ_0 is a constant, $E_{max}(T)$ is the impurity state energy and $E_h(T)$ is the hopping energy of the charge

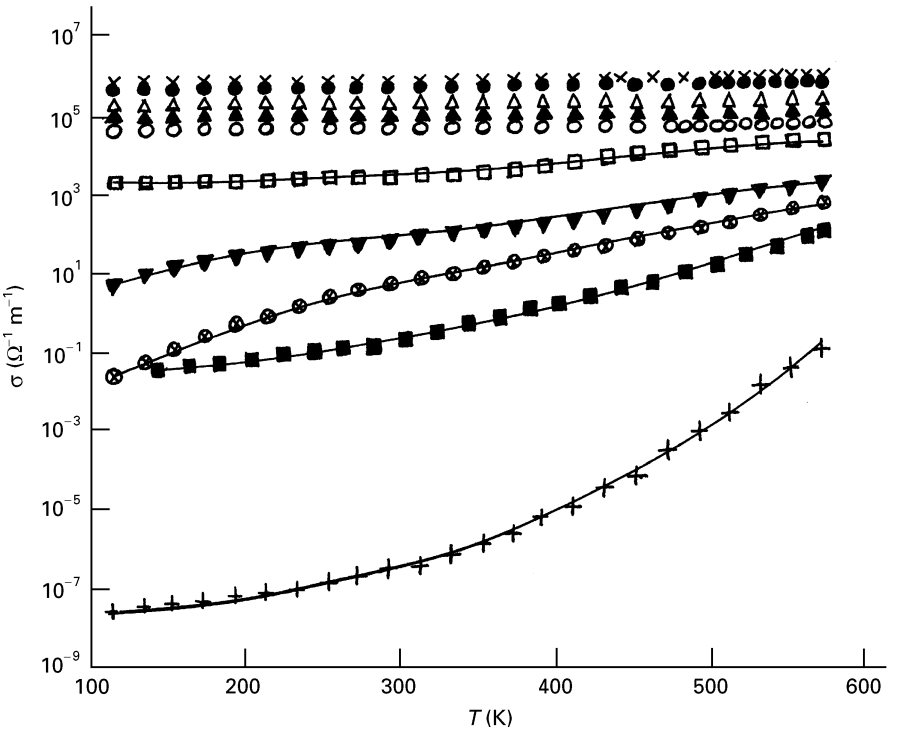

Figure 3 Variation of d.c. conductivity with temperature for: + 3 at % Mn, ■ 10 at % Mn, ⊗ 20 at % Mn, ▼ 40 at % Mn, □ 50 at % Mn, ○ 60 at % Mn, ▲ 70 at % Mn, △ 80 at % Mn, ● 90 at % Mn, × 100 at % Mn.

carriers. The conduction mechanism may be described qualitatively by invoking the dominant-current model [19]. This assumes that the largest contribution to the d.c. conductivity at a temperature T arises from localized states situated at an energy $E_{max}(T)$ away from the Fermi level.

5. Conclusion

Three conduction mechanisms have been identified in Mn/SiO_x thin films: p-type, intrinsic and metallic. The thermoelectric power activation energy E_s and d.c. activation energy E_σ enables the positive charge carriers to be classified as nonpolaronic holes and small polarons in the temperature range 275 to 460 K. Conduction depends critically upon metallic content. Below 60 at % Mn, conduction is activated and the films have an island structure whereas above 60 at % Mn, conduction is non-activated, and the structure is filamentary.

References

1. J. BEYNON, *Thin Solid Films* **37** (1976) L71.
2. J. BEYNON and N. R. P. MILWAY, *ibid.* **14** (1972) 387.
3. S. K. J. AL-ANI, M. A. R. SARKAR and J. BEYNON, *J. Mater. Sci.* **20** (1985) 1737.
4. M. R. RAHIM, PhD thesis, Brunel University, UK (1994).
5. H. HEIKES and R. W. URE, "Thermoelectricity: Science and Engineering" (Interscience, New York, 1961) p. 311.
6. L. J. van der PAUW, *Philips Res. Rep.* **13** (1958) 1.
7. E. CROSSMAN, A. GRILL and M. POLLAK, *Thin Solid Films* **119** (1984) 349.
8. T. L. BARR, "Modern ESCA, The Principles and Practice of X-Ray Photoelectron Spectroscopy" (CRC Press Inc., Boca Raton, FLa., London, 1994) pp. 22, 93.
9. S. Z. A. ZAIDI, B. R. ORTON and J. BEYNON, *Phys. Status. Solidi* **158** (1996) p. K1.
10. F. BUCHY, M. T. CLAVAGUERA and P. H. GERMAIN, "Conduction in Low Mobility Materials", edited by N. Klein, D. S. Tannhauser and M. Pollak (Taylor and Francis, London, 1971) p. 23.
11. H. J. GOLDSMID, "Thermoelectric Refrigeration" (Temple Press Books Ltd., London, 1964) p. 38.
12. C. B. STEELE and J. BEYNON, *Thin Solid Films* **213** (1992) 76.
13. D. K. C. MACDONALD, "Thermoelectricity: An Introduction to the Principles" (J. Wiley & Sons Ltd., New York, 1992) p. 114.
14. S. Z. A. ZAIDI, J. BEYNON, C. B. STEELE and B. R. ORTON, *Thin Solid Films* **256** (1995) 120.
15. B. DONOVAN, "Elementary Theory of Metals" (Pergamon Press, Oxford, 1967) p. 190.
16. N. F. MOTT and E. A. DAVIS, "Electronic Processes in Non-Crystalline Materials", 2nd edition (Clarendon Press, Oxford,1979) pp. 33, 65–97, 199, 235.
17. C. B. STEELE, J. BEYNON and C. A. HOGARTH, *J. Phys. C* **20** (1987) L617.
18. C. KITTEL, "Introduction to Solid State Physics" (J. Wiley & Sons Ltd., New York, 1986) p. 24.
19. R. M. HILL, *J. Phys. C* **5** (1972) L267.

Received 18 October
and accepted 19 November 1996